Pure & Appl. Chem., Vol. 60, No. 2, pp. 215–221, 1988.
Printed in Great Britain.

Photochemistry of organometallics: potential energy surfaces and reaction mechanisms

Alain Veillard, Chantal Daniel and Alain Strich

E.R. 139 du CNRS, Institut Le Bel, 4 rue Blaise Pascal, 67000 Strasbourg, France

Abstract - Configuration interaction calculations, based on Complete Active Space SCF wavefunctions, are reported for the lowest excited states of $Fe(CO)_5$, $HMn(CO)_5$ and $HCo(CO)_4$. Potential energy curves have been computed at the same level of accuracy for the photodissociation of $HCo(CO)_4$. The mechanism of the photochemical reactions of these organometallics is discussed. The cis stereospecificity of the photosubstitution of d^6 metal carbonyls is explained on the basis of state correlation diagrams.

INTRODUCTION

There is an extensive photochemistry of organometallics (ref. 1). As noted in a recent review, "one unfortunate characteristics of much of organometallic photochemistry is a relative absence of detailed mechanistic information. Without such information the systematic and rationally planned use of photochemical techniques and the exploitation of photochemical intermediates are left largely to chance" (ref. 2). Current understanding (ref. 1) has been based on molecular orbital diagrams coupled with an analysis in terms of bonding and antibonding character, with the assumption that exciting an electron from a bonding to the corresponding antibonding orbital should result in photodissociation. This approach fails for instance to interpret the photosubstitution of CO in iron tricarbonyl di- and tetraazabutadiene complexes, since the calculations do not show any change in metal-CO bonding in the lowest excited states (ref. 3). It is unable to explain the occurence of competitive photochemical reactions at a given wavelength, such as the simultaneous photolytic cleavage of the metal-hydrogen and photochemical loss of a carbonyl ligand reported for $HCo(CO)_4$, or the concurrent cleavage of the metal-metal bond and loss of a carbonyl ligand found in the photochemistry of $Mn_2(CO)_{10}$ (ref.2 and 4).

A deep understanding of photochemical reactions requires a knowledge of the potential energy surfaces (PES) which connect the reactants to the primary photochemical products. Whenever potential energy surfaces are not available, one may rely on their qualitative counterparts, the state correlation diagrams (Ref. 5). We have been engaged, for the last few years, in the derivation of state correlation diagrams and in the calculation of potential energy curves for representative phochemical reactions of organometallics (Ref. 6-12). We present here a survey of the methodology and of the results.

METHODOLOGY

The method used should reproduce correctly the sequence and energetics of electronic states of the reactant and products. For this reason the SCF method is generally not appropriate for the calculation of PES, since it frequently leads to errors of 1 eV or more in the calculated excitation energies (Ref. 13). Configuration interaction (CI) based on SCF reference wavefunctions gives results which are qualitatively correct in general, however accurate results may require very long CI expansions (ref. 9). The CASSCF (Complete Active Space SCF) method (Ref. 14) has been used to obtain reference wavefunctions and orbitals for the calculation of excited states of $Fe(CO)_5$ and $HMn(CO)_5$ and of the PES for $HCo(CO)_4$. These CASSCF calculations were followed by contracted CI (CCI calculations) (ref. 15).

The rigorous way to calculate excitation energies and potential energy surfaces consists of carrying out for each electronic state a CASSCF calculation followed by a contracted CI calculation (ref. 16). However this method becomes too expensive for the studies reported here. The approach which we have used consists of performing a CASSCF calculation for a particular state and using this CASSCF reference wavefunction for the CCI calculations of all the states of interest (Ref. 12). The choice of this particular state was dictated by the following considerations. The ground state is not the best candidate, since the CCI calculations would be biased in favour of this state and would

lead to overestimated excitation energies. Whenever possible, we have selected a state with an occupation number close to one for the orbitals which are empty in the ground state but populated in the low-lying excited states. Details of these CASSCF calculations are given in Table 1. For $Fe(CO)_5$, the occurence of symmetry breaking solutions forced us to rely on a CASSCF wavefunction optimized for the ground state.

TABLE 1. The CASSCF calculations

	State	Principal Configuration	Active Space[a]	Nb. of electrons in active space
$Cr(CO)_6$	$^7A_{1g}$	$t_{2g}^3 e_g^2 a_{1g}^1$	$3d(t_{2g},e_g),4s$	6
	$^1A_{1g}$	t_{2g}^6	$3d(t_{2g},e_g),4d(t_{2g})$	6
$HMn(CO)_5$	$^5A_2$	$d_{xy}^2 d_\pi^2 \sigma^2 \sigma^{*1} d_{x^2-y^2}^1$	$3d,4d_{xy},4d_\pi,\sigma,\sigma^*$	8
	$^1A_1$	$d_{xy}^2 d_\pi^4 \sigma^2$	"	8
$Fe(CO)_5$	$^1A_1$	$d_\pi^4 d_\sigma^4$	$3d,4d_\pi,4d_\sigma$	8
$HCo(CO)_4$	$^3A_1$	$d_\sigma^4 \sigma^1 \sigma^{*1}$	$3d_\sigma,4d_\sigma,\sigma,\sigma^*$	6

[a] σ and σ^* denote the m.o.'s which are bonding and antibonding with respect to the metal-hydrogen bond.

For each electronic state, two CCI calculations were performed. The first one has only one reference configuration while the second one is a multireference calculation. The reference configurations of the second one are the configurations with a coefficient greater than a given threshold (usually between 0.08 and 0.065) in the wavefunction of the first calculation. The number of reference configurations selected in this way was between 2 and 10. The number of electrons correlated was 6 in $Cr(CO)_6$, 8 in $HMn(CO)_5$ and $Fe(CO)_5$ (namely the 3d electrons and the 2 electrons of the Mn-H bond in $HMn(CO)_5$) and 6 in $HCo(CO)_4$ (the $3d_\sigma$ electrons and the 2 electrons of the Co-H bond). The calculations included single and double excitations to all virtual orbitals except the counterparts of the carbonyl 1s and of the metal 1s, 2s and 2p orbitals. The number of configurations ranged from 38000 to 317000 for $HMn(CO)_5$ and from 183000 to 509000 for $HCo(CO)_4$ but this number was reduced to at most a few thousands by the contraction.

The following gaussian basis sets were used : for the transition metal a (15,11,6) set contracted to [9,6,3] (ref. 17), for the first row atoms a (10,6) set contracted to [4,2] (ref. 18) and for hydrogen a (6,1) set contracted to [3,1] (ref. 19). This basis set is triple-zeta for the 1s shell of hydrogen and for the 3d and 4s shells of the transition atoms, otherwise it is double-zeta.

The calculations for $Cr(CO)_6$, $HMn(CO)_5$, $Fe(CO)_5$ and $HCo(CO)_4$ were performed for the experimental geometry of these molecules (ref. 20-22). For the calculation of the potential energy curves of $HCo(CO)_4$, we have assumed that C_{3v} symmetry was retained along the reaction path since both $Co(CO)_4$ and $HCo(CO)_3$ have been found to have C_{3v} symmetry in their ground state (ref. 10 and 23).

The integral and SCF calculations were carried out either with the system of programs ASTERIX (ref. 24) or with the system of programs ARGOS (ref. 25). The CASSCF and CCI calculations were performed with the system SWEDEN (ref. 26).

CALCULATION OF EXCITED STATES

One major difficulty in the calculations of excited states is due to the fact that organometallics are characterized by the occurence of a large number of excited states within a relatively narrow energy region. For instance 18 excited states were located between 33000 and 51000 cm^{-1} for $Fe(CO)_5$ (ref. 9). Another difficulty arises when one wants to compare the calculated excitation energies to experimental values, since the electronic spectra of organometallics are poorly resolved in general (certainly as a consequence of this high density of states). These electronic spectra show usually a broad band (corresponding generally to a charge transfer transition) with one or two shoulders (see for instance ref. 1, 27 and 28). Since our interest centers mostly on the ligand field (LF), $d \rightarrow \sigma^*$ and $\sigma \rightarrow \sigma^*$ excitations which turn out to be responsible of the photochemical reactions studied here, we have not in general calculated the many metal-to-ligand charge-transfer (MLCT) excited states corresponding to the $d \rightarrow \pi^*_{CO}$ excitations or the Rydberg type excited states (corresponding to the $3d \rightarrow 4d$, 5s, 5p excitations). We shall review briefly the main results.

$Fe(CO)_5$

The LF excited states $^1E'$ and $^1E''$ are calculated respectively at 33400 and 34100 cm^{-1} (ref. 12). Since these excitation energies were obtained with a CASSCF reference wavefunction optimized for the ground state, they are probably overestimated by about 5000 cm^{-1} as judged from the results obtained for the LF states of $HMn(CO)_5$ with different reference wavefunctions (Table 2). This would put the LF state $^1E'$ at about 28000-29000 cm^{-1}. This is in good agreement with the experimental spectrum which shows a very weak absorption in the region of 28600 cm^{-1} (ref. 29).

$HMn(CO)_5$

The calculated excitation energies are shown in Table 2. The $^3A_1$ $\sigma \rightarrow \sigma^*$ excitation is computed at 46900 cm^{-1}. One $3d_{xy} \rightarrow 4d_{xy}$ transition, calculated at 49000 cm^{-1}, may correspond to a Rydberg transition (although this 4d orbital is localized in the same region of space as the 3d orbitals), in good agreement with the fact that excitation to the 4d level starts at 47000 cm^{-1} for the Mn atom (ref. 30). The experimental spectrum of $HMn(CO)_5$ in the gas phase shows one broad band around 46700 cm^{-1} with two shoulders at 34500 and 51300 cm^{-1}, these three features having been assigned as MLCT transitions (ref. 28). According to the results of Table 2, the transition at 34500 cm^{-1} should rather correspond to the LF excitations. This assignment is supported by the low value of the intensity in the experimental spectrum, a general feature of the LF transitions. The intense band at 46700 cm^{-1} corresponds probably to several transitions such as the $d_\pi \rightarrow \sigma^*$, $3d \rightarrow 4d$ and MLCT transitions (the allowed transition $^1A_1 \rightarrow {}^1E$ corresponding to the $d_\pi \rightarrow \sigma^*$ excitation is computed at 42300 cm^{-1}).

TABLE 2. Calculated excitation energies (in cm^{-1}) for $HMn(CO)_5$

State	One-electron excitation in the principal configuration		
$^3A_2$	$d_{xy} \rightarrow d_{x^2-y^2}$	27600	
^3E	$d_\pi \rightarrow d_{x^2-y^2}$	25200	
$^3A_1$	$\sigma \rightarrow \sigma^*$	46900	
$^1A_2$	$d_{xy} \rightarrow d_{x^2-y^2}$	33300	(38700[b])
^1E	$d_\pi \rightarrow d_{x^2-y^2}$	33700[a]	(42100[b])
^1E	$d_\pi \rightarrow \sigma^*$	42300[a]	
$^1B_2$	$d_{xy} \rightarrow \sigma^*$	53000	
$^1A_1$	$d_{xy} \rightarrow 4d_{xy}$	49000[a]	
$^1A_2$	$d_{xy} \rightarrow \pi^*$	53600	
$^1A_1$	$\sigma \rightarrow \sigma^*$	61800[a]	

[a] Symmetry allowed.
[b] From a CAS-SCF wavefunction optimized for the ground state.

$HCo(CO)_4$

A $^3A_1$ state corresponding to the $\sigma \rightarrow \sigma^*$ excitation is computed at 34600 cm^{-1}. The ^3E and ^1E states corresponding to the $d_\sigma \rightarrow \sigma^*$ excitation are calculated at 25900 and 36000 cm^{-1} respectively. The absorption spectrum of $HCo(CO)_4$ shows an intense band at 44000 cm^{-1} corresponding certainly to a CT transition (Ref. 4), with the weaker $d_\sigma \rightarrow \sigma^*$ transition probably buried under it.

MECHANISM OF PHOTOCHEMICAL REACTIONS

Photodissociation of $Fe(CO)_5$

The mechanism which we have proposed for the primary step of the photodissociation of $Fe(CO)_5$

$$Fe(CO)_5 \xrightarrow{h\nu} Fe(CO)_4 + CO$$

is based on state correlation diagrams and potential energy curves (ref. 6 and 9) which show that a single potential energy surface connects, without any barrier, the LF state $^3E'$ of $Fe(CO)_5$ to the ground state $^3B_2$ of the products $Fe(CO)_4$ + CO. This mechanism is represented in Fig. 1. Excitation to the LF state $^1E'$ is followed by intersystem crossing to the state $^3E'$. From there the molecule dissociates to the products of the reaction along the $^3B_2$ potential energy surface (assuming that C_{2v} symmetry is retained along the reaction path). The conclusion that the LF excited state $^3E'$ correlates with the ground state of the products is independant of the assumptions made on the dissociating ligand (equatorial or axial) and on the symmetry retained along the reaction path (ref. 9). This mechanism has been used to interpret the results of laser photolysis experiments on $Fe(CO)_5$ in the gas phase (ref. 31).

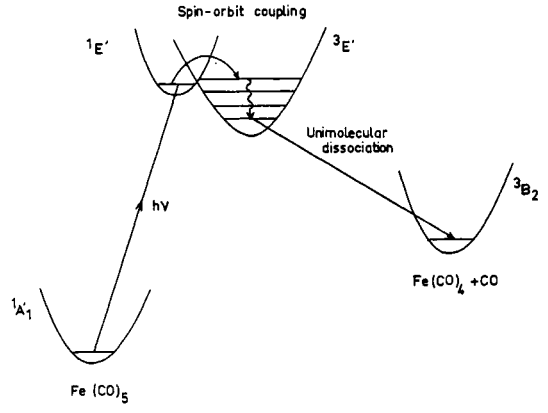

Fig. 1. The mechanism proposed for the photochemical dissociation of $Fe(CO)_5$.

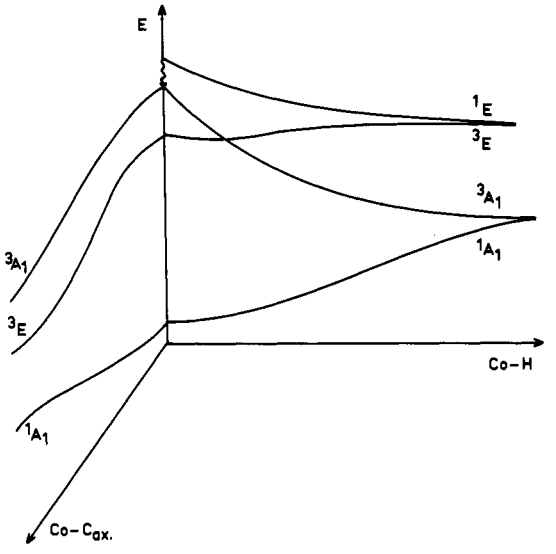

Fig. 2. Potential energy surfaces for the ground and excited states of $HCo(CO)_4$.

Photochemistry of $HCo(CO)_4$

Irradiation of $HCo(CO)_4$ at 254 nm (39400 cm^{-1}) results in two photochemical reactions corresponding respectively to the loss of a carbonyl ligand and to the homolysis of the cobalt-hydrogen bond :

$$HCo(CO)_4 \xrightarrow{h\nu} HCo(CO)_3 + CO$$

$$HCo(CO)_4 \xrightarrow{h\nu} Co(CO)_4 + H$$

Potential energy surfaces for the ground and excited states of $HCo(CO)_4$ (Fig. 2) have been inferred from the potential energy curves calculated for the loss of either the hydrogen or the axial carbonyl ligand (Ref. 23). These surfaces form the basis for a qualitative understanding of the photochemistry of $HCo(CO)_4$. We propose that irradiation at 254 nm brings the molecule into the ^1E state (corresponding to the $d_\sigma \rightarrow \sigma^*$ excitation and calculated at 36000 cm^{-1}), this being followed by intersystem crossing to the $^3A_1$ $\sigma \rightarrow \sigma^*$ state (calculated at 34600 cm^{-1}). From there the molecule may evolve along three different channels corresponding to :

i) the dissociation of the Co-H bond along the $^3A_1$ curve, with formation of the products H and $Co(CO)_4$ in their ground state ;

ii) the loss of a carbonyl ligand along the $^3A_1$ curve, forming the products CO and $HCo(CO)_3$ in the excited state $^3A_1$;

iii) the formation of the products CO and $HCo(CO)_3$ in the excited state ^3E by crossing from the $^3A_1$ to the ^3E surface.

We predict that chemiluminescence should be observed for the photochemical decarbonylation in the gas phase (chemiluminescence has been predicted and observed for the photodecarbonylation of $Ni(CO)_4$, Ref. 9 and 32).

Photochemistry of $HMn(CO)_5$

Depending on the wavelength, the photolysis of $HMn(CO)_5$ results either in carbonyl loss (at 229 nm or 43700 cm^{-1})

$$HMn(CO)_5 \xrightarrow{h\nu} HMn(CO)_4 + CO$$

or in hydrogen loss (at 193 nm or 51800 cm^{-1})

$$HMn(CO)_5 \xrightarrow{h\nu} Mn(CO)_5 + H$$

In the absence of potential energy surfaces for this system, any proposal for a mechanism should be viewed as tentative. The mechanism which we propose for hydrogen dissociation is based on a state correlation diagram (Ref. 7) and is similar to the one advanced for $HCo(CO)_4$. Irradiation at 51800 cm^{-1} to a singlet state is followed by intersystem crossing to the $^3A_1\ \sigma \rightarrow \sigma^*$ state (calculated at 46900 cm^{-1}). From there the molecule dissociates along the $^3A_1$ potential energy curve to the products H and $Mn(CO)_5$ in their ground state. As to the photochemical loss of a carbonyl ligand observed at 43700 cm^{-1}, we tentatively propose that it results from excitation to the $^1E\ d_\pi \rightarrow \sigma^*$ state (calculated at 42300 cm^{-1}) since the potential energy curve for the $^3E\ d_\sigma \rightarrow \sigma^*$ of $HCo(CO)_4$ is dissociative with respect to the loss of a carbonyl ligand (Fig. 2).

Photosubstitution of d^6 metal carbonyls

Photosubstitution of monosubstituted d^6 metal carbonyls $M(CO)_5L$ may result in CO labilization and this reaction has been found to be highly stereospecific, yielding the cis isomer (references may be found in Ref. 11, see also Ref. 33) :

$$M(CO)_5L+L' \xrightarrow{h\nu} \text{cis-}M(CO)_4LL' + CO$$

This reaction is the result of a photoelimination followed with a nucleophilic reaction :

$$M(CO)_5\,L \xrightarrow{h\nu} M(CO)_4L + CO$$

$$M(CO)_4\,L + L' \longrightarrow M(CO)_4\,LL'$$

SCF and CI calculations have been used to generate state correlation diagrams for the primary photoelimination (Ref. 11). Fig. 3 represents the state correlation diagram for the photoelimination of the axial carbonyl ligand from $M(CO)_5$ L. On the basis of this diagram, we have proposed the following mechanism for the photosubstitution of the axial carbonyl :

i) excitation of $M(CO)_5L$ into the ^1E LF state is followed by elimination of the carbonyl ligand with the species $M(CO)_4$ L formed in the excited state ^1E as a square pyramid with the ligand L apical ;

ii) $M(CO)_4$ L evolves along a Berry pseudorotation path first to a trigonal bipyramid in the $^1B_2$ state then to a square pyramid with L basal in the $^1A'$ excited state ;

iii) $M(CO)_4$ L being trapped in the potential well corresponding to this excited state $^1A'$ can evolve only through internal conversion to the ground state $^1A'$;

iv) $M(CO)_4$ L being trapped as a square pyramid with L basal in the potential well of the ground state $^1A'$ can only react with an incident nucleophile to give $M(CO)_4LL'$ with the cis structure (Scheme 1).

Scheme 1

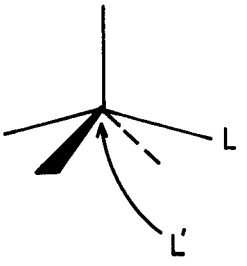

A similar analysis leads to the same conclusion for the photoelimination of an equatorial carbonyl ligand, namely that the product $M(CO)_4LL'$ should be formed with the cis structure (Fig. 4). This analysis may also be extended (Ref. 11) to account for the stereospecificity observed in the photochemistry of $M(CO)_4(L)$ where the ligand L occupies two cis coordination sites, as found in $Mo(CO)_4$(dppe) with the photosubstitution resulting in the sole production of fac-[$Mo(CO)_3$(dppe)L] (Ref. 34) or in the (η^4-diene)$Cr(CO)_4$ complexes, with the photolysis resulting in the formation of fac-(η^4-diene)$Cr(CO)_3$ (Réf. 35).

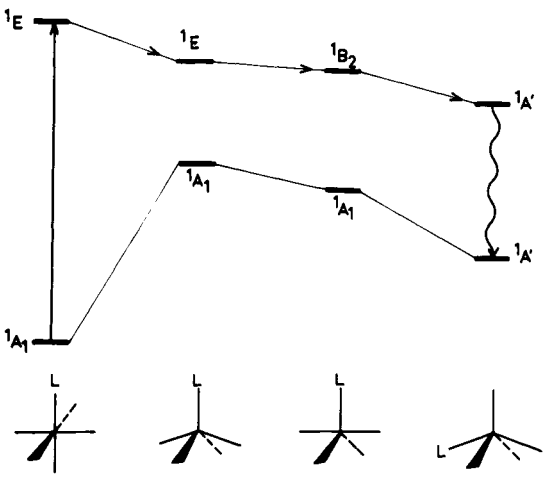

Fig. 3. State correlation diagram for the photoelimination of the axial carbonyl ligand from $M(CO)_5L$ (this ligand does not appear in the diagram for the sake of clarity).

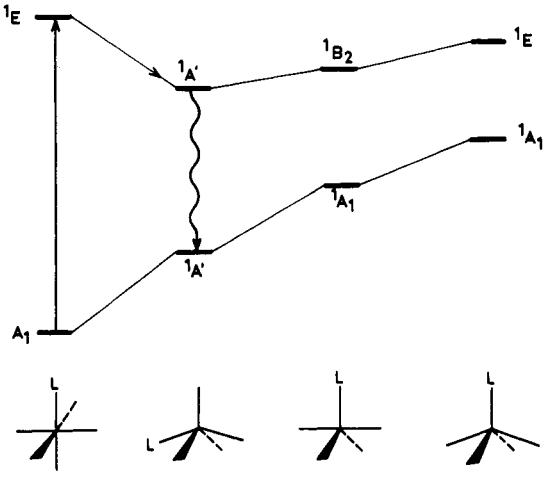

Fig. 4. State correlation diagram for the photoelimination of an equatorial carbonyl ligand from $M(CO)_5L$.

Photochemistry of peroxometalloporphyrin complexes

The photolysis of the peroxometalloporphyrin complexes $Ti(O_2)(TPP)$ and $Mo(O_2)(TPP)$ gives rise to evolution of O_2 in the $^1\Delta_g$ excited state (Ref. 36) :

$$M(O_2)(TPP) \xrightarrow{h\nu} M(TPP) + O_2$$

A state correlation diagram, based on SCF calculations for the reactant (Ref. 37) is shown in Fig. 5. The excited state $^1A_1$ of the reactant corresponds to the electronic configuration $Ti(II)O_2$ $d^2(\pi_g^a)^2(\pi_g^b)^0$ (where π_g^a and π_g^b denote the π_g orbitals of dioxygen which are respectively symmetrical and antisymmetrical with respect to the plane defined by the Ti atom and the O_2 ligand) It correlates through an avoided crossing with the products TiP and O_2 in the $^1\Delta_g$ state, providing a rationale for the experimental findings.

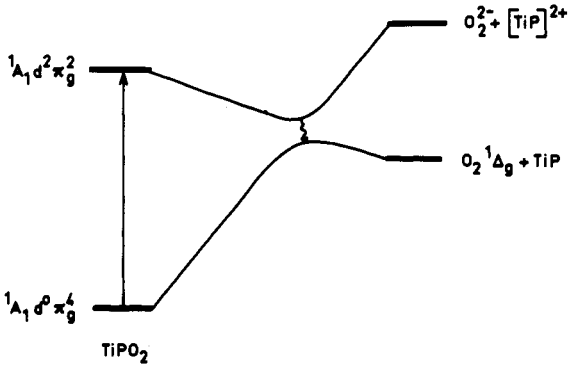

Fig. 5. State correlation diagram for the photoelimination of dioxygen from $TiPO_2$ (P = porphine dianion).

CONCLUSION

The calculation of potential energy surfaces (or potential energy curves) and the construction of state correlation diagrams has enabled us to get a better understanding of the mechanism of these photochemical reactions. The importance of intersystem crossing from a singlet state (reached through excitation of the reactant) to a triplet state (which connects to the ground state of the products) has become clear in the

photochemistry of $Fe(CO)_5$ and $HCo(CO)_4$. It certainly represents a general mechanism for the photochemical homolysis of a σ bond and could be extended to the photochemical cleavage of the metal-carbon bond in $RMn(CO)_5$, of the metal-silicon bond in $R_3SiCo(CO)_4$ and of the metal-metal bond in dinuclear complexes like $Mn_2(CO)_{10}$. The occurence of different reactive channels in the photochemistry of $HCo(CO)_4$ results from the crossing of two potential energy surfaces, both dissociative.

Acknowledgements

We are grateful to Prof. P.E.M. Siegbahn for making available the program SWEDEN and to Prof. R.M. Pitzer for the program ARGOS. The calculations have been carried out on the CRAY-1 of the CCVR (Palaiseau) through a grant of computer time from the Conseil Scientifique du Centre de Calcul Vectoriel pour la Recherche.

REFERENCES

1. G.L. Geoffroy and M.S. Wrighton, Organometallic photochemistry, Academic Press, New-York (1979).
2. T.J. Meyer and J.V. Caspar, Chem. Rev. 85, 187-218 (1985).
3. W.C. Trogler, in Excited states and reactive intermediates, A.B.P. Lever ed., p. 177, American Chemical Society, Washington (1986).
4. R.L. Sweany, Inorg. Chem., 21, 752-756 (1982).
5. See for instance N.J. Turro, Modern Molecular photochemistry, Benjamin, Menlo Park, California, 1978.
6. A. Veillard, Nouv. J. Chim., 5, 599-601 (1981).
7. A. Veillard and A. Dedieu, Nouv. J. Chim., 7, 683-686 (1983).
8. A. Veillard and A. Dedieu, Theoret. Chim. Acta, 63, 339-348 (1983).
9. C. Daniel, M. Bénard, A. Dedieu, R. Wiest and A. Veillard, J. Phys. Chem., 88, 4805-4811 (1984).
10. C. Daniel, I. Hyla-Kryspin, J. Demuynck and A. Veillard, Nouv. J. Chim., 9,581-590 (1985).
11. C. Daniel and A. Veillard, Nouv. J. Chim., 10, 83-90 (1986).
12. A. Veillard, A. Strich, C. Daniel and P. Siegbahn, submitted for publication.
13. M. Bénard, J. Demuynck, M.-M. Rohmer and A. Veillard, in Spectroscopie des éléments de transition et des éléments lourds dans les solides, Colloques Internationaux du CNRS n° 255, Paris, 1977.
14. P.E.M. Siegbahn, J. Almlof, A. Heiberg and B.O. Roos, J. Chem. Phys., 74, 2384-2396 (1981).
15. P.E.M. Siegbahn, Intern. J. Quantum Chem., 23, 1869-1889 (1983).
16. See for instance J. Matos, B. Roos and P. Malmqvist, J. Chem. Phys., 86, 1458-1466 (1987).
17. A.J.H. Wachters, J. Chem. Phys., 52, 1033-1036 (1970).
18. S. Huzinaga, Approximate atomic functions, Technical Report, University of Alberta, Alberta, 1971.
19. S. Huzinaga, J. Chem. Phys., 42, 1293-1302 (1965).
20. B. Rees and A. Mitschler, J. Am. Chem. Soc., 98, 7918-7924 (1976).
21. E.A. McNeill and F.R. Scholer, J. Am. Chem. Soc., 99, 6243-6249 (1977).
22. B. Beagley and D.G. Schmidling, J. Mol. Struct., 22, 466-468 (1974).
23. A. Veillard and A. Strich, to be published.
24. M. Bénard, A. Dedieu, J. Demuynck, M.-M. Rohmer, A. Strich, A. Veillard and R. Wiest, unpublished.
25. R.M. Pitzer, J. Chem. Phys., 58, 3111-3112 (1973).
26. P.E.M. Siegbahn, C.W. Bauschlicher, B. Roos, A. Heiberg, P.R. Taylor and J. Almlof, SWEDEN, a MCSCF - direct CI.
27. M. Dartiguenave, Y. Dartiguenave and H.B. Gray, Bull. Soc. Chim. Fr., 4223-4225 (1969).
28. G.B. Blakney and W.F. Allen, Inorg. Chem., 10, 2763-2770 (1971).
29. J.T. Yardley, B. Gitlin, G. Nathanson and A.M. Rosan, J. Chem. Phys., 74, 370-378 (1981).
30. C.E. Moore, Atomic energy levels, Circular 467, National Bureau of standards, 1952.
31. T.A. Seder, A.J. Ouderkirk and E. Weitz, J. Chem. Phys., 85, 1977-1986 (1986).
32. N. Rosch, H. Jorg and M. Kotzian, J. Chem. Phys., 86, 4038-4045 (1987).
33. B.H. Weiller and E.R. Grant, J. Am. Chem. Soc., 109, 1252-1253 (1987).
34. G. Andolfatto, R. Granger and L.K. Peterson, Inorg. Chim. Acta, 99, L1-L3 (1985).
35. W. Gerhatz, F.W. Grevels, W.E. Klotzbucher, E. von Gustorf and R.N. Perutz, Z. Naturforsch., 40b, 518-523 (1985).
36. P. Bergamini, S. Sostero, O. Traverso, P. Deplano and L.J. Wilson, J.C.S. Dalton Trans., 2311-2314 (1986).
37. M.-M. Rohmer, M. Barry, A. Dedieu and A. Veillard Int. J. Quant. Chem., Quant. Biol. Symp., 4, 337-342 (1977).